3.7.7 Crystallographic description for C18 and C19

As shown in the figures 40 and 41, the overall geometry of **C18** and **C19** can be regarded as octahedron, with the equatorial plane defined by the imine nitrogen, phenoxyl oxygen, sulfur atom and one of the terminal oxygen atoms of the dioxomolybdenum. The other terminal oxygen and the nitrogen or oxygen atom from the bridging 4, 4'-bipyridine or 4, 4'-bipyridine *N, N'*-dioxide molecules occupy the apical position. The two oxygen atoms, a sulfur, a nitrogen and the molybdenum atom are found to be essentially coplanar, in which the molybdenum atom show a slight shift out (0.2764 Å and 0.2358 Å) from the basal plane towards the O3 direction. Typical values for the O=Mo=O angles are around 108°, while optimal values for Mo=O distance lies around 1.70 Å.

The Mo – D (donor atom of solvent) bond length in the dioxomolybdenum(VI) complexes are generally found somewhat longer than the normal single bond length due to the consequence of the *trans* effect of M=O_t (where O_t is oxo-group *trans* to the Mo – $O_{solvent}$). In these cases, the Mo – N(3) distance (2.4566 Å) is longer than that of Mo – O(4) (2.297 Å). This result reveals a rather weak attachment of 4,4-biypridine ligands compared to 4,4'-bipyridine N,N'-dioxide to the MoO_2^{2+} moiety.

A closer look into the crystal structure packing of **C18** shows that the supramolecular rectangular structure of **C18** has been constructed by intermolecular hydrogen bonding interaction, N7-H7A….O3 as shown in table 34 and figure 47. The oxo-group is engaged in the H-bond interaction with hydrogen atom attached at N7 atom from the neighboring molecule, with the result that the chains are interlocked into two dimensional polymeric network which runs along the *bc*- crystallographic plane (fig.48). On the contrary, the hydrogen atom from the secondary amine group of one **C19** molecule form a hydrogen bond to a nitrogen atom of the 4,4'-bipyridine of the adjacent **C19** molecules (Fig.49). This arrangement gives rise to the formation of a one-dimensional helical chain that runs along the diagonal of *ac* crystallographic plane (table 35 & Fig.50).

Table 34: Hydrogen bonds in **C18** [Å and °].

D-H...A	d(D-H)	d(H...A)	d(D...A)	<(DHA)
N(3)-H(3)...O(6)#1	0.86	2.09	2.9278(17)	165.6
N(7)-H(7A)...O(3)#2	0.86	2.19	3.0466(16)	175.3

Symmetry codes:
#1 x+1/2,-y+3/2,z+1/2 #2 x-1/2,-y+1/2,z-1/2

Table 35: Hydrogen bonds in **C19** [Å and °].

D-H...A	d(D-H)	d(H...A)	d(D...A)	<(DHA)
N(3)-H(3A)...O(4)#	0.86	2.21	2.959(3)	145.5

Symmetry code: #-x,-y+2,-z+2

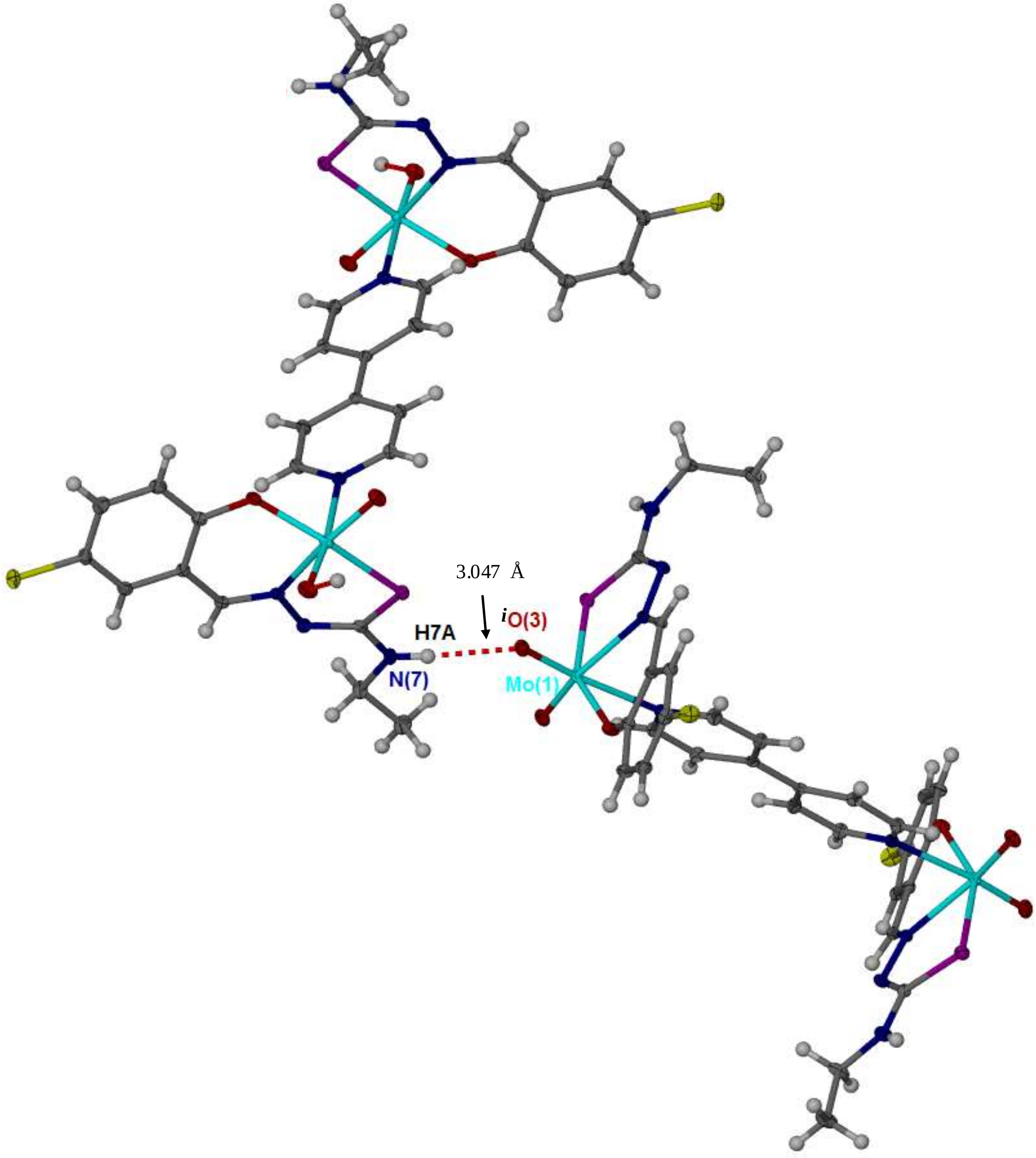

Figure 47: Intermolecular hydrogen bonds in the crystal structure of C18
Symmetry code (i): x-1/2,-y+1/2,z-1/2

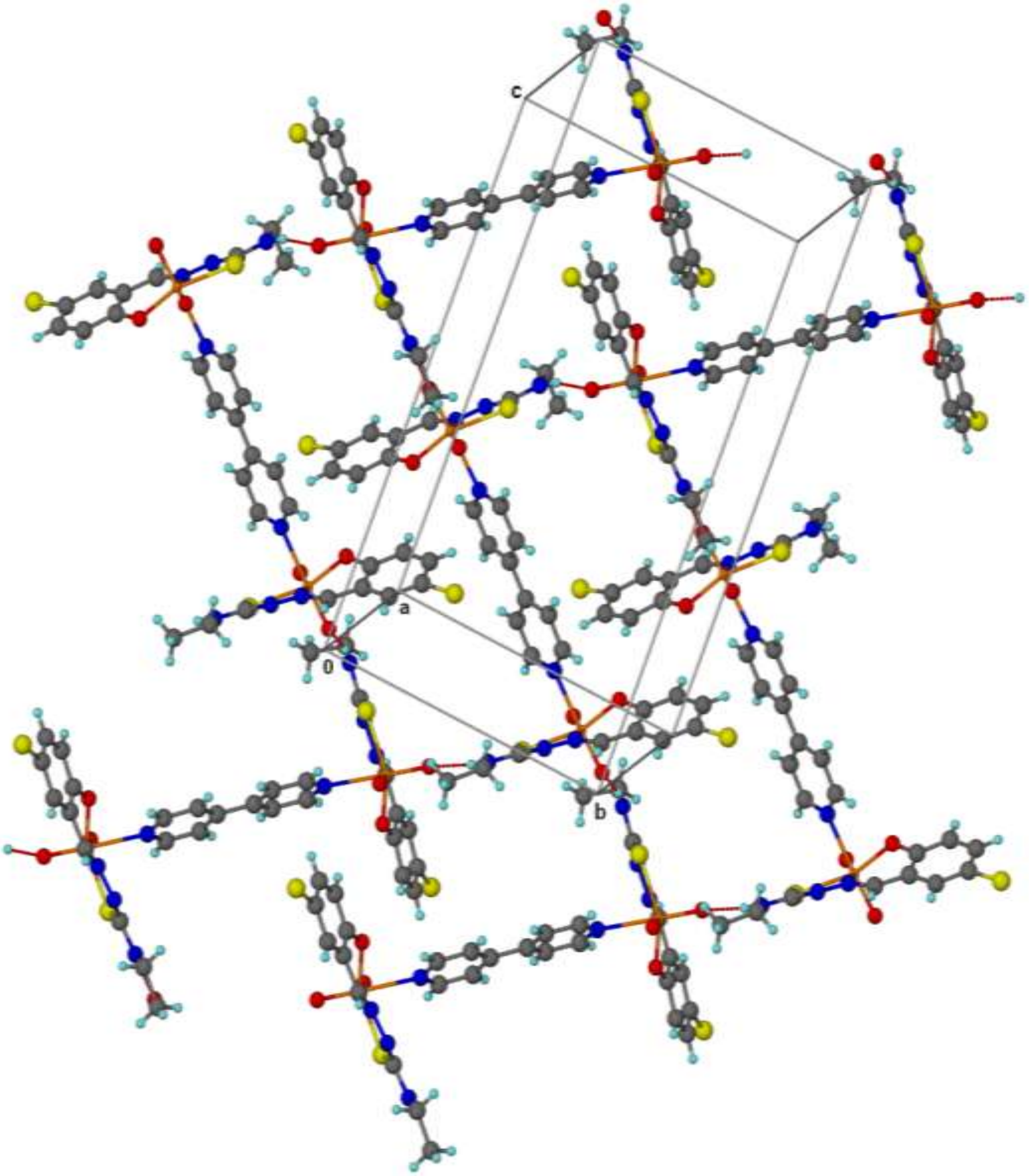

Figure 48: Interlocking of chain assembled by hydrogen bonding in C18 viewed along the *a*-axis

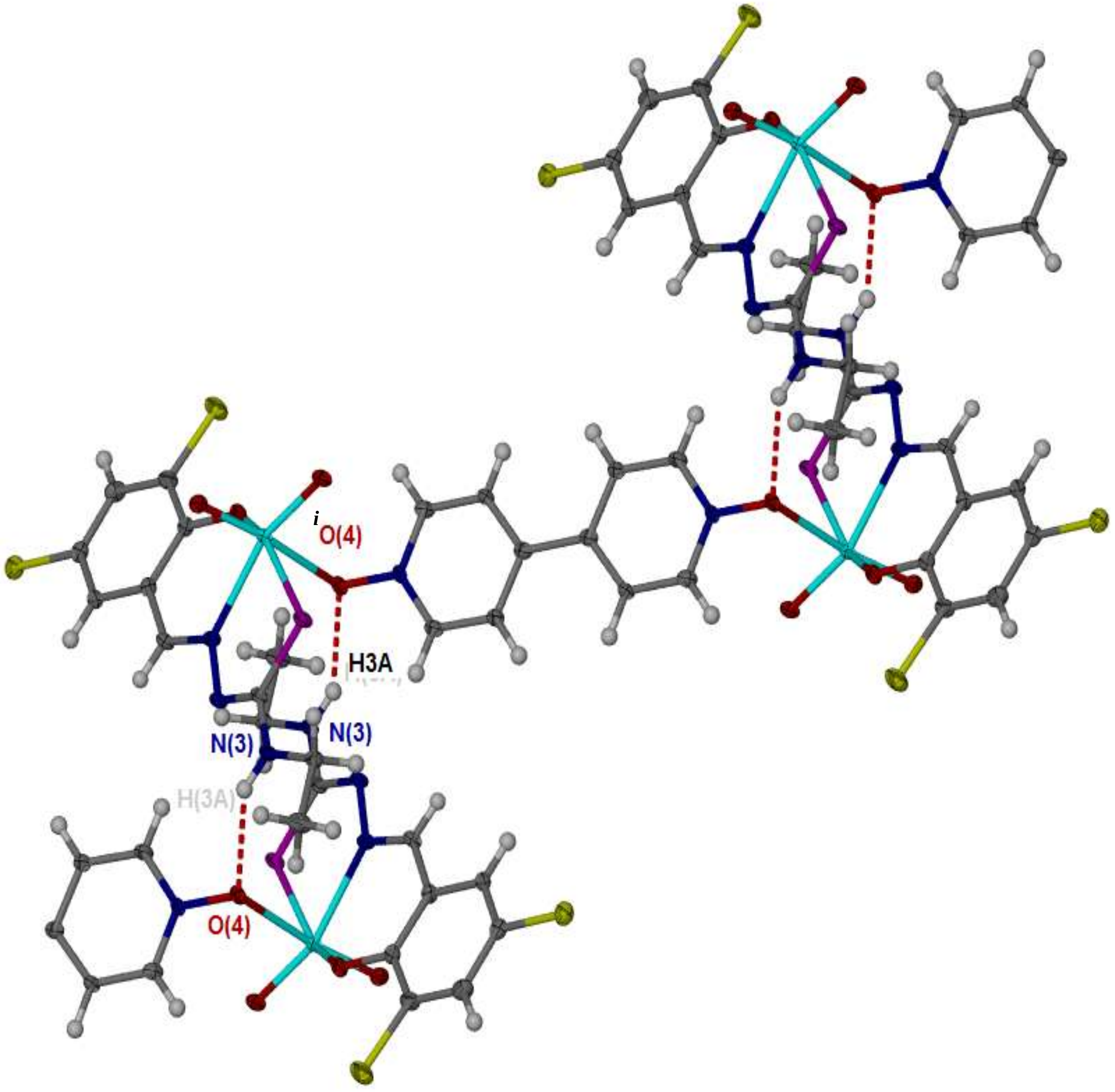

Figure 49: Intramolecular hydrogen bonds in the crystal structure of C19.

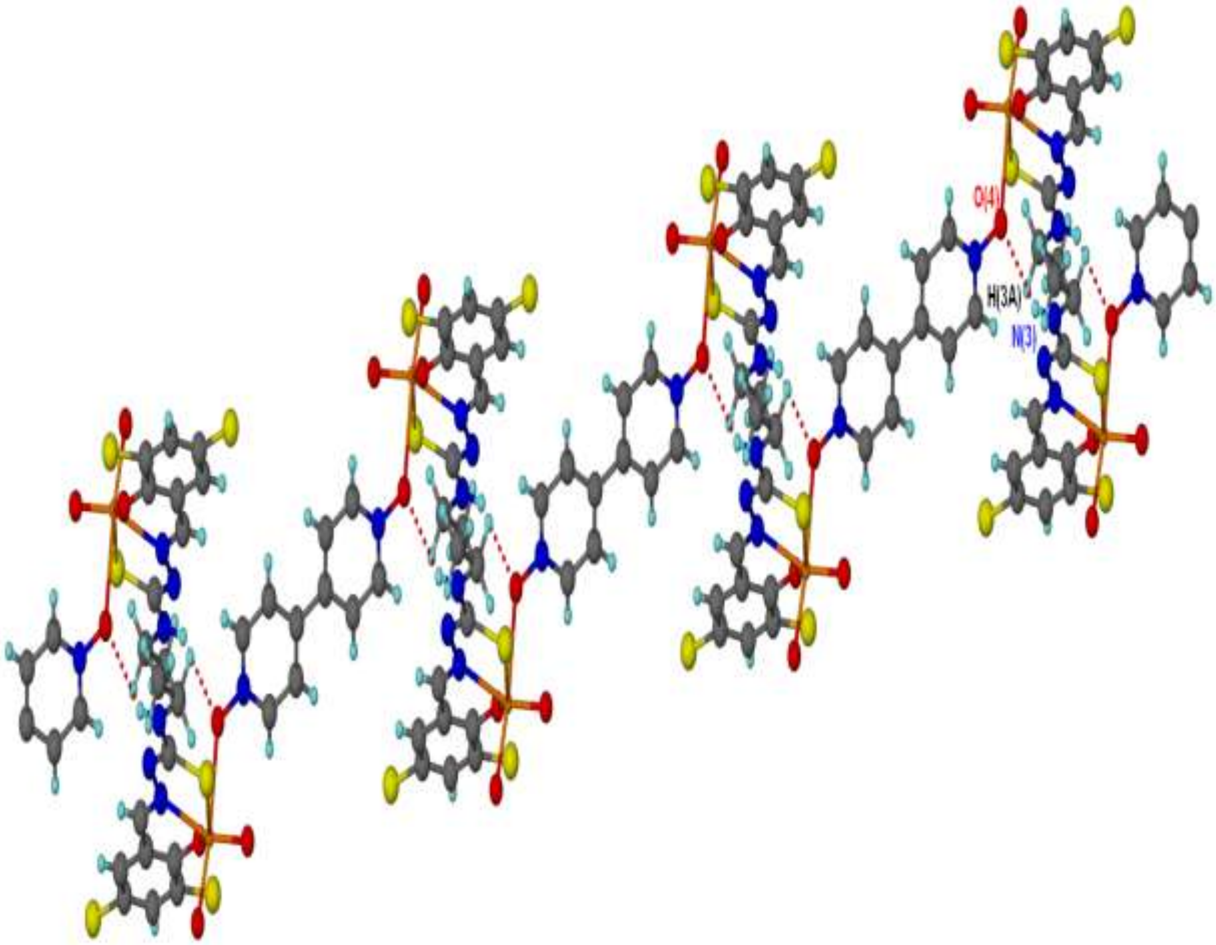

Figure 50: X-ray crystal structure of C19 showing the arrangement of molecules into hydrogen bonded polymeric helical chain.

3.7.8 Crystallographic description for C20-C23

The structures of **C20-C23** consist of $(MoO_2)L$, accompanying two unit of donor solvent molecules. Unlike **C18** and **C19**, the octahedral environment around molybdenum atom comprises of *cis*-Mo = O, imine nitrogen, phenoxyl oxygen and hydroxyl oxygen from the enolized carbonyl group, further supported by monodentate neutral ligands such as ethanol, DMF and HMPA. The average values for Mo-O(2)/(3) distance and O=Mo=O angle in these complexes varies slightly in 1.70-1.72 Å and in 104-107^{o}, respectively. On the other hand, least-square calculation shows that the molybdenum atoms of **C22** deviates the least (0.2118Å) toward the distal O3, indicating that the deviation is restricted by the presence of HMPA bulky molecule in the complex. The planarity of this equatorial plane was further corroborated by the close linearity of the O2-Mo-N1 angle of **C22**, 162.16(12) Å.

Table 36: Hydrogen bonds in **C20** [Å and ^{o}]

D-H...A	d(D-H)	d(H...A)	d(D...A)	<(DHA)
O(6)-H(1)...N(2)#	0.62(4)	2.18(4)	2.798(3)	172(5)

Symmetry code: # -x,-y+1,-z+2

Table 37: Hydrogen bonds in **C21** [Å and ^{o}]

D-H...A	d(D-H)	d(H...A)	d(D...A)	<(DHA)
O(5)-H(1)...N(2)#	0.70(3)	2.01(3)	2.710(2)	177(3)

Symmetry code: # -x+2,y,-z+1/2

The extended structure of **C20-C23** revealed that the butylene chains of these structures adopted the antiperiplanar or *zigzag* conformation (figs. 42, 44, 45 and 46) except for **C21** in which the butylene chain adopts the gauche staggered conformation (table 37 and Fig. 43). In this case, the two dioxomolybdenum fragments rotate about the C-C bond of the butylene chain to facilitate the intramolecular O-H…N hydrogen bonding between the ethanol donor ligand and the imino nitrogen of the Schiff base (fig.51). In the case of the complex containing the ethanol molecule **C20**, adjacent molecules are linked by OH·····N hydrogen bonds into a polymeric chain that runs along the *a*-axis of the monoclinic unit cell (table 36 and fig.52). Since there is no evidence of hydrogen bonding interaction or C-H …. π weak interaction in the crystal structures, **C22** and **C23** exists as discrete molecules.

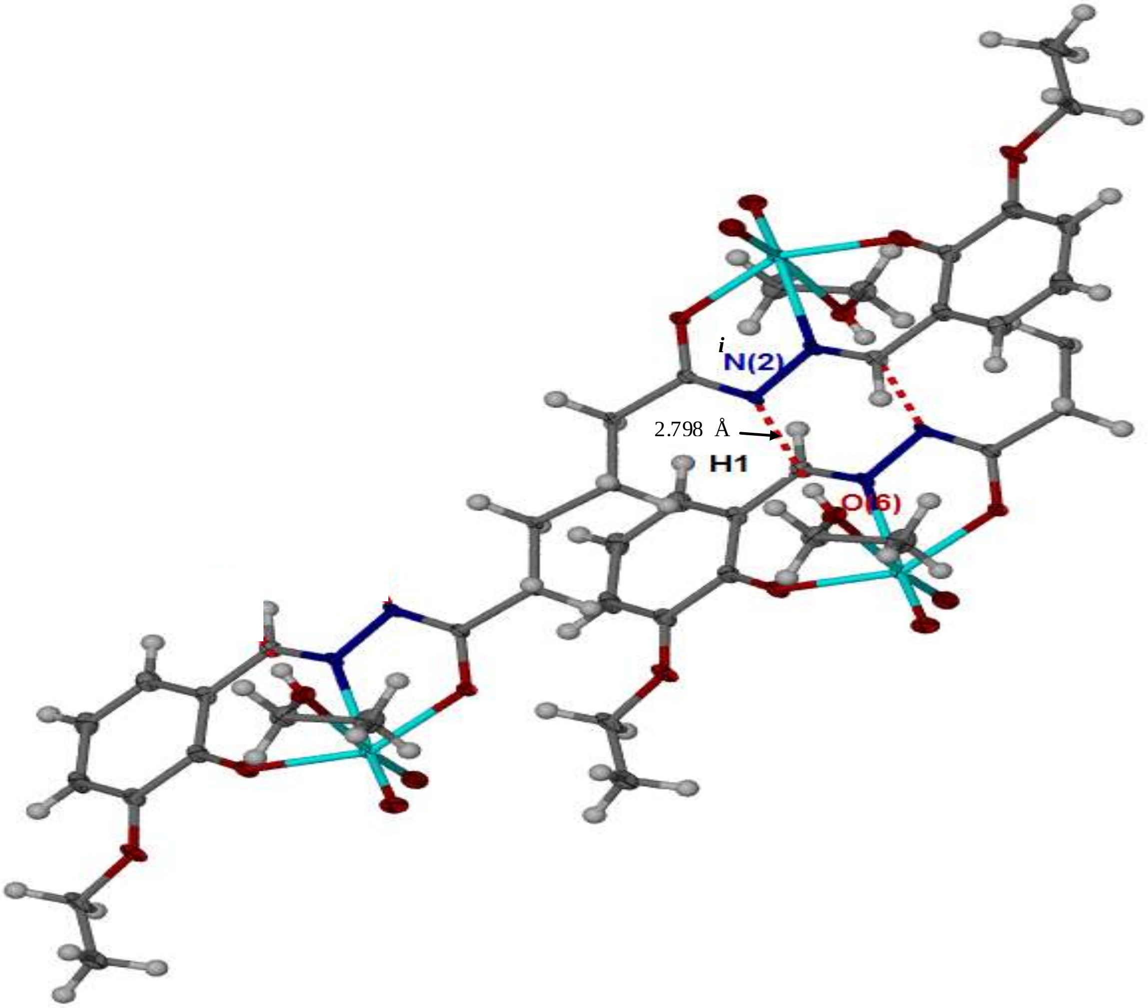

Figure 51: Intermolecular hydrogen bonds in the crystal structure of C20. Symmetry code(i): -x,-y+1,-z+2.

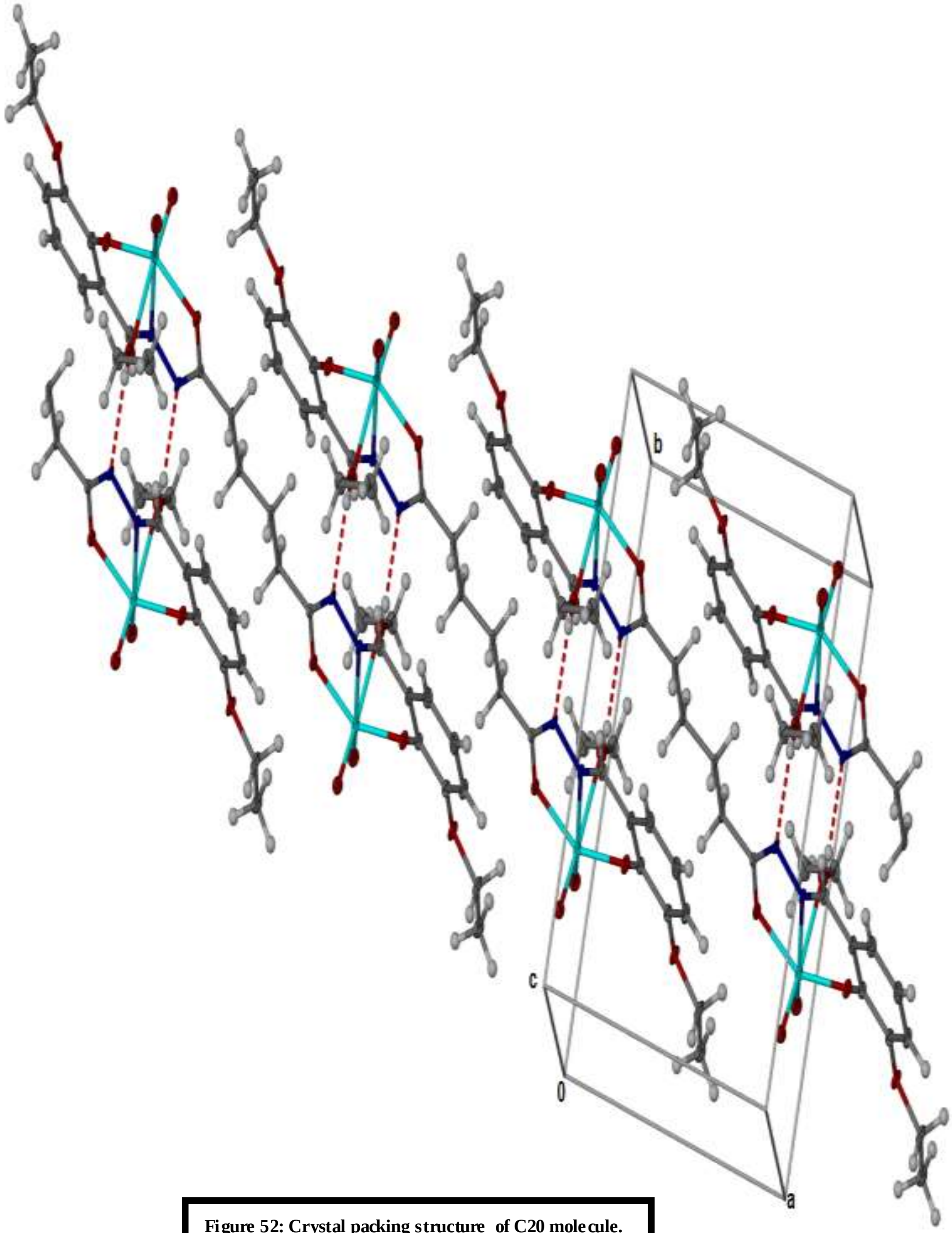

Figure 52: Crystal packing structure of C20 molecule.

3.7.9 Crystallographic description for C24

The reaction between 1,4-bis(4-hydroxysalicylaldehyde carbohydrazonato)butane and $MoO_2(acac)_2$ in the presence of 4,4'-bipyridine yielded **C24.** Crystal structure of the compound consist of 1D *zig-zag* chain in which the binuclear *cis*-dioxomolybdenum(VI) fragments are linked covalently by 4,4'-bipyridine bidentate ligand. The adjacent chains are further interconnected through O5-H5…O2 hydrogen bond interaction leading to the formation of highly ribbed two dimensional lamella framework with open void (table 38). The methanol molecules are involved in hydrogen bonding to the terminal oxygen of molybdenum atom (O3) and fill the space between the ligands. The bipyridine plane (N3-C11-C12-C13-C14-C15) and the Mo1-O4-C8-N2-N4 plane lies at 78^{o} to one another to fabricate supramolecular staircase running infinitely along the *a*-axis. The present of additional –OH substituent group in dihydrozone ligand that act as potential subunit for the formation of supramolecular staircase through self-assembly of conformational rigid molecular scaffold help to stabilize the overall molecular structure (fig. 53&54) [81].

Table 38: Hydrogen bonds in **C24** [Å and ^{o}].

D-H...A	d(D-H)	d(H...A)	d(D...A)	<(DHA)
O(5)-H(5)...O(2)#1	0.84	1.97	2.805(4)	173.6
O(6)-H(6A)...O(3)#2	0.84	2.04	2.725(6)	138.4

Symmetry codes: #1 x-1,y,z; #2 x+1,y,z

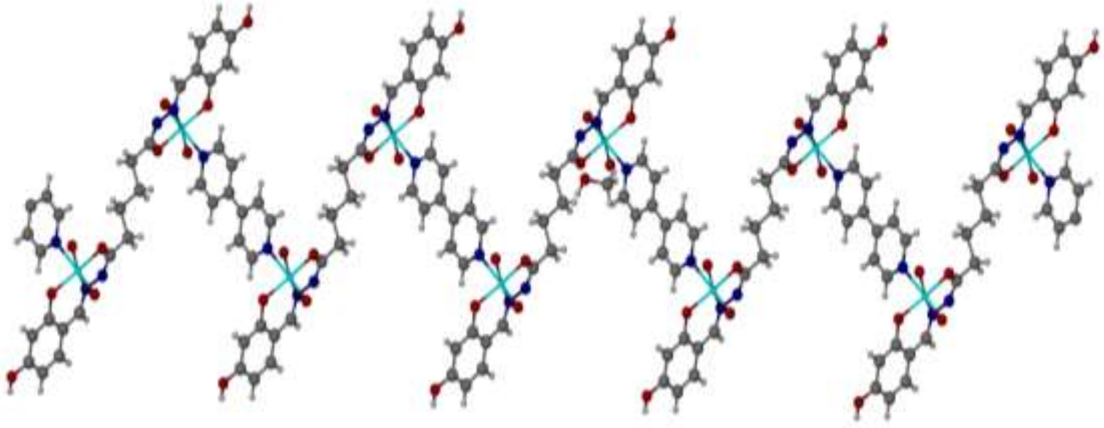

Figure 53: The picture of coordinative bond between the 4,4'-bipyridine and the molybdenum atom along the one dimensional chain of the title complex.

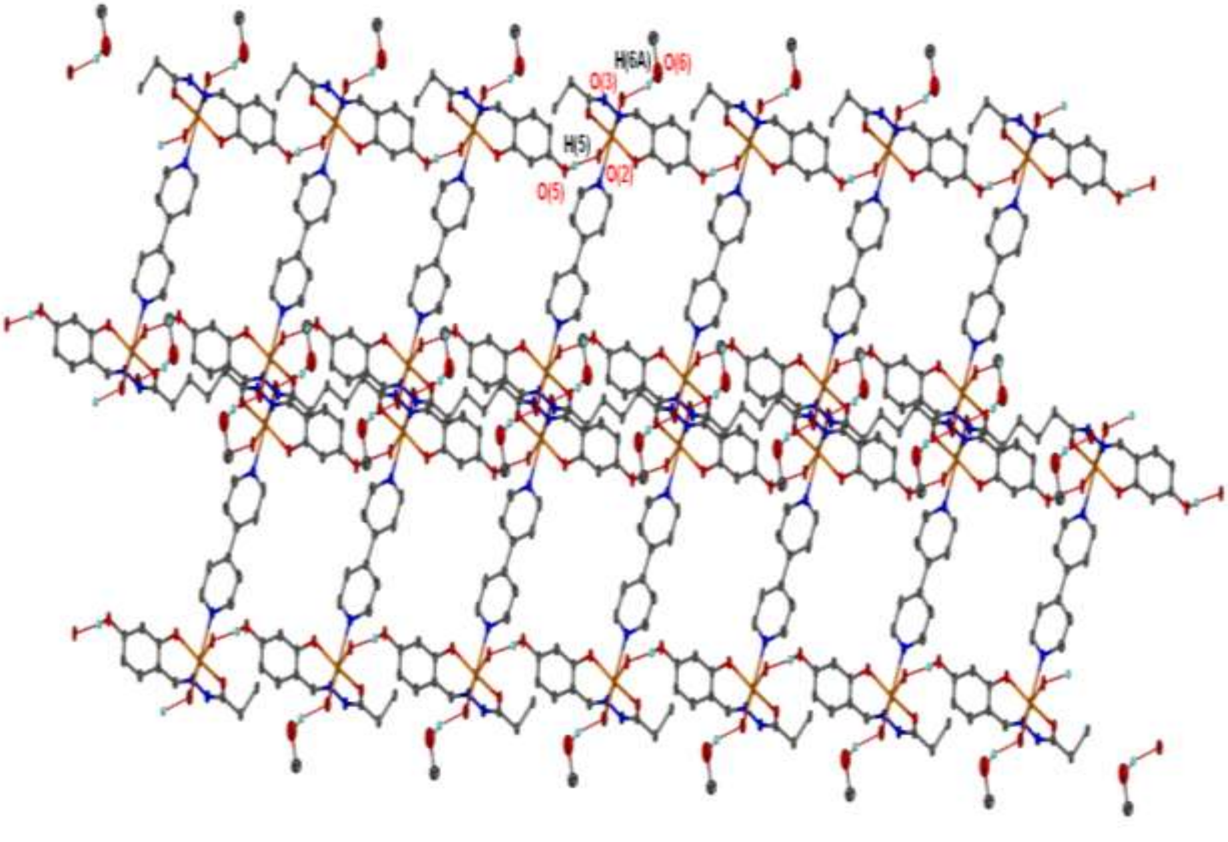

Figure 54: Inter-chains hydrogen bonds in C24.

3.8 Catalytic Property of Dioxomolybdenum(VI) Complexes: Oxidation of Alcohol

3.8.1 Oxidation of Alcohol with Hydrogen Peroxide Catalyzed by Some Cis Dioxomolybdenum(VI) Tridentate Schiff Base Complexes.

Table 39: Screening for Suitable Catalyst for Oxidation of Alcohol after 24 hours

Reactants/ Catalyst	**Cal. Mass/g**	**Molar Mass / $gmol^{-1}$**	**Cal. Mole**	**Mole fraction (%)**	**% Conversion Benzyl alcohol**
$C_6H_5CH_2OH$	10.40	108.14	0.10	49.80	-
H_2O_2	3.33	34.01	0.10	49.80	-
Without Catalyst	-	-	-	-	0.00
Without H_2O_2	-	-	-	-	0.00
C4	0.55	552.00	0.001	0.40	3.10
C10	0.52	518.00	0.001	0.40	4.80
C11	0.62	619.00	0.001	0.40	4.00
C12	0.51	513.00	0.001	0.40	3.30
C13	0.54	539.00	0.001	0.40	28.30
C14	0.54	544.00	0.001	0.40	7.60
C16	0.62	621.00	0.001	0.40	10.70
C17	0.57	572.00	0.001	0.40	11.10
C18	0.92	923.00	0.001	0.40	26.30
C19	1.03	1026.00	0.001	0.40	12.40
C20	0.81	814.00	0.001	0.40	9.10
C21	0.87	866.00	0.001	0.40	10.30
C22	1.08	1082.00	0.001	0.40	5.50
C23	0.87	868.00	0.001	0.40	5.50
C24	0.45	445.00	0.001	0.40	40.20

Volume of benzyl alcohol used: 10.00 cm^3
Volume of 30% H_2O_2 used : 3.00 cm^3
Density of benzyl alcohol : 1.04 gcm^{-3}
Density of 30% H_2O_2 : 1.11 gcm^{-3}

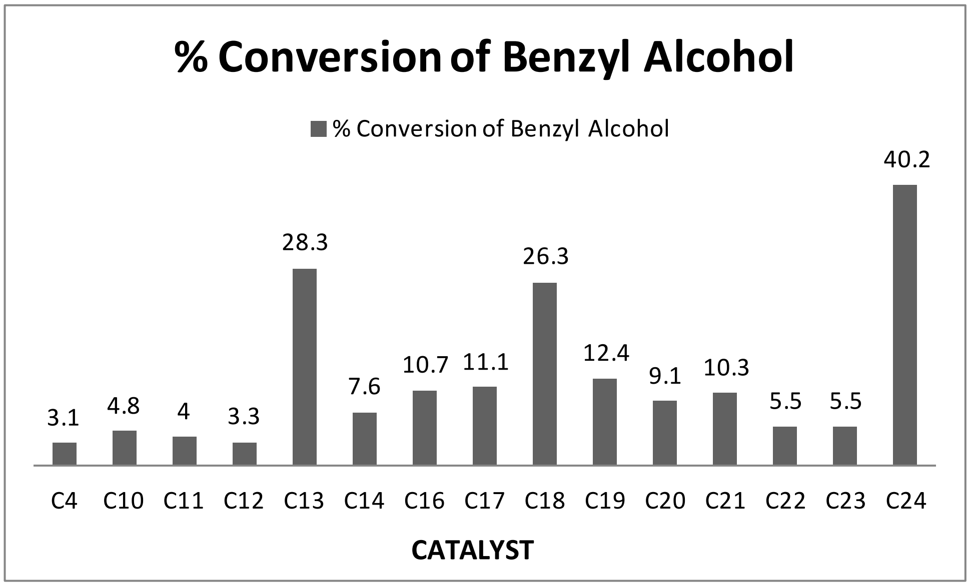

Figure 55: Oxidation Reaction Catalyzed by Different Type of Dioxomolybdenum(VI) Complexes. Reaction Condition: Molar ratio of $C_6H_5CH_2OH/H_2O_2$ = 1:1; 0.001 mol of catalysts. Temperature at 90°C for 24 hours.

3.8.2 Description of Oxidation Reaction Catalyzed by Different Types of Dioxomolybdenum(VI) Complexes

The result presented in the table 39 and figure 55 are referring to the percentage of conversion of benzyl alcohol to benzoic acid with different dioxomolybdenum(VI) complexes. Catalytic oxidation reaction yields benzoic acid as the product only after 24 hours of reaction. Blank runs are performed and as expected, without catalyst, no significant benzoic acid has been observed under the applied condition, indicating the catalytic ability of the complexes. The observations were repeated here indicate that **C13, C18** and **C24** in which the sixth coordinating site of Mo(VI) ion is occupied with 4,4-bipyridine give higher activity and performance to the oxidation of alcohol. It was also found that the percentage of alcohol conversion for the rest of the oxomolybdenum(VI) complexes within 24 hours is about 10%. In other words the catalytic action is preliminary and shows the compounds to be only limitedly active and do not contribute much to catalytic action as no significant conversion was observed. The difference found in the level of conversion is probably due to the nature of the ligands that coordinate to the Mo centre. Record has shown that the efficacy of a great catalyst depends on the metal as well as the surrounding ligands providing the steric and electronic environment that influence the performance of the catalyst. According to Jia Li *et.al.*, dioxomolybdenum(VI) complexes using two connected bridging ligands containing nitrogen donor such as 4,4'-bipyridine are found to be good catalyst for oxidation and epoxidation process using H_2O_2 as oxidant [73b]. The amine additive such as pyridine, pyrazole, and 3-cyanopyridine enhance the efficiency of catalytic oxidation [82-87]. The aromatic N-base ligands work by coordinating to the molybdenum center, thereby reducing the Lewis acidity of the catalyst and additionally accelerating the catalytic reaction [88-89].

3.8.3 Influence of Catalyst Loading on Oxidation of Alcohol

Calculation of the mole ratio of $C_6H_5CH_2OH/H_2O_2$ and the catalysts concentration used.

Mass of $C_6H_5CH_2OH$ = 10.44 g

Mass of H_2O_2 = 3.33 g

Mole ratio $C_6H_5CH_2OH/H_2O_2$ = 1:1

Table 40: Preparation of Catalyst

Catalyst	**Cal. Mass/g**	**Molar Mass / $gmol^{-1}$**	**Cal. Mole**	**Mole fraction(%)**
C13	0.54	540.00	0.0010	0.40
	1.08		0.0020	0.80
	1.35		0.0025	1.20
C18	0.92	923.00	0.0010	0.40
	1.85		0.0020	0.80
	2.32		0.0025	1.20
C24	0.45	445.00	0.0010	0.40
	0.90		0.0020	0.80
	1.11		0.0025	1.20

Table 41: Conversion of benzyl alcohol to benzoic acid using 1.0, 2.0 and 2.5 mmol of **C13**

Time/ hours	**Percentage of Conversion (%)**		
	1.0 mmol	**2.0 mmol**	**2.5 mmol**
0	0	0	0
24	28.30	40.30	40.50
36	40.20	60.50	65.00
48	60.00	88.30	88.00
60	89.20	89.00	90.40

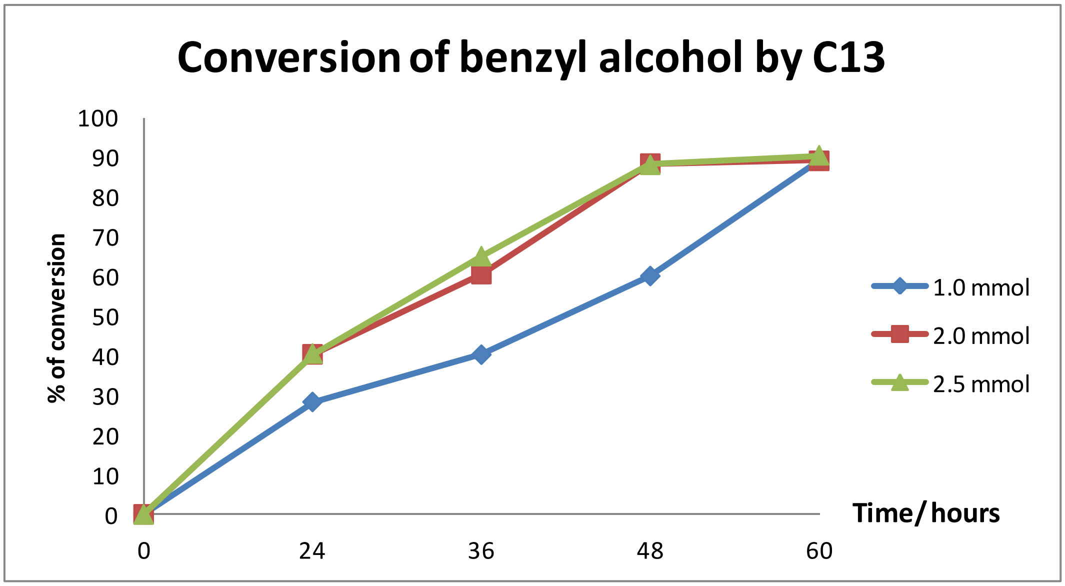

Figure 56: Conversion of benzyl alcohol to benzoic acid using 1.0, 2.0 and 2.5 mmol of C13

Table 42: Conversion of benzyl alcohol to benzoic acid using 1.0, 2.0 and 2.5 mmol of **C18**.

Time/ hours	**Percentage of Conversion (%)**		
	1.0 mmol	**2.0 mmol**	**2.5 mmol**
0	0	0	0
24	26.30	46.10	45.70
36	45.40	62.60	65.00
48	65.00	85.10	86.00
60	85.70	90.20	89.30

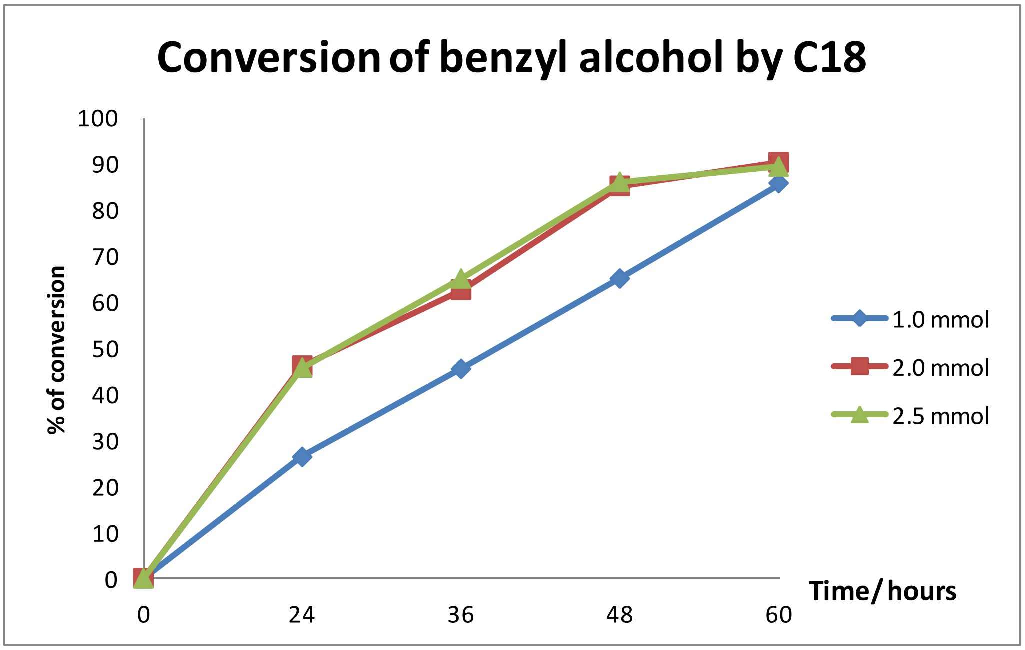

Figure 57: Conversion of benzyl alcohol to benzoic acid using 1.0, 2.0 and 2.5 mmol of C18

Table 43: Conversion of benzyl alcohol to benzoic acid using 1.0, 2.0 and 2.5 mmol of **C24**

Time/ hours	**Percentage of Conversion (%)**		
	1.0 mmol	**2.0 mmol**	**2.5 mmol**
0	0	0	0
24	40.20	44.10	45.80
36	60.60	70.60	65.10
48	79.00	85.50	86.20
60	87.90	88.70	89.00

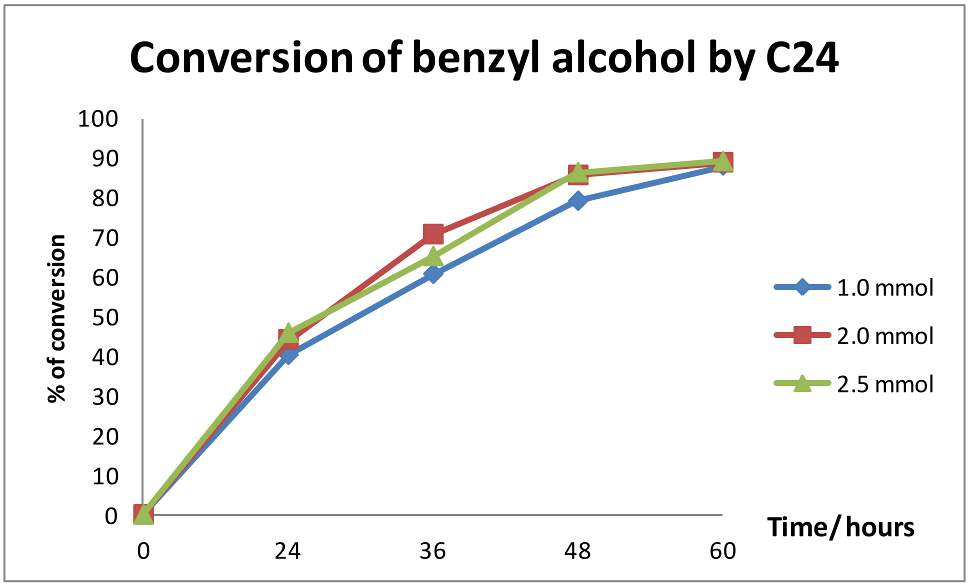

Figure 58: Conversion of benzyl alcohol to benzoic acid using 1.0, 2.0 and 2.5 mmol of C24

Description of the Influence of Catalyst Loading

Since **C13**, **C18** and **C24** were found to give higher catalytic activity and performance to the oxidation of alcohol, the effect of catalysts concentration of these three catalyst was further studied. The reactions were carried out with the molar ratio $C_6H_5CH_2OH/H_2O_2$ is 1:1 and the reaction temperature is 90^oC with vigorous stirring. All the reactions achieved 90% benzyl alcohol conversion after 60 hours (table 41-43). In the case of **C13** and **C18**, an amount of 1.0 mmol of the catalysts produces 90% of benzoic acid after 60 hours while it took only 48 hours only using 2.0 and 2.5 mmol of the catalysts to achieve the same result. This result indicates faster conversion of benzyl alcohol was obtained with higher loading of catalyst. However, there is no further improvement when the amount of catalyst was increased from 2.0 to 2.5 mmol, indicating that a concentration level of 2.0 mmol (0.8% by number of mol) is sufficient for benzyl alcohol to achieve 90% conversion within 48 hours. In the case of **C24**, varying the catalyst loading from 1.0 mmol to 2.5 mmol gave similar amount of conversion. However, in comparison with **C13** and **C18**, the catalytic performance of **C24** towards the oxidation of alcohol is higher as 80% of benzyl alcohol conversion can be achieved with 1.0 mmol (0.4% by mol) of catalyst.

3.8.4 Influence of Concentration of Substrate

Table 44: Molar ratio of the substances

Reactants/ Catalyst	**Cal. Mass/g**	**Molar Mass / gmol^{-1}**	**Cal. Mole/**	**Mole ratio $C_6H_5CH_2OH/H_2O_2$**
$C_6H_5CH_2OH$	10.44	108.14	0.100	1:1
	20.88		0.200	2:1
	31.32		0.300	3:1
H_2O_2	3.33	34.01	0.100	49.60
C13	1.08	540.00	0.002	-
C24	0.90	445.00	0.002	-

Table 45: Conversion of benzyl alcohol using **C13** and **C24**

Time/hours	% of conversion using **C13**			% of conversion using **C24**		
	1:1	**2:1**	**3:1**	**1:1**	**2:1**	**3:1**
0	0	0	0	0	0	0
24	40.30	43.30	45.00	44.10	46.60	48.00
36	60.50	62.50	65.40	70.60	72.60	74.00
48	88.30	90.00	91.30	85.50	90.40	92.00
60	89.00	92.70	93.50	88.70	92.00	94.00

Reaction condition:
1:1, 2:1, 3:1 are the molar ratio of $C_6H_5CH_2OH/H_2O_2$; amount of catalyst used is 2.0 mmol and the reaction temperature is 90 ^oC.

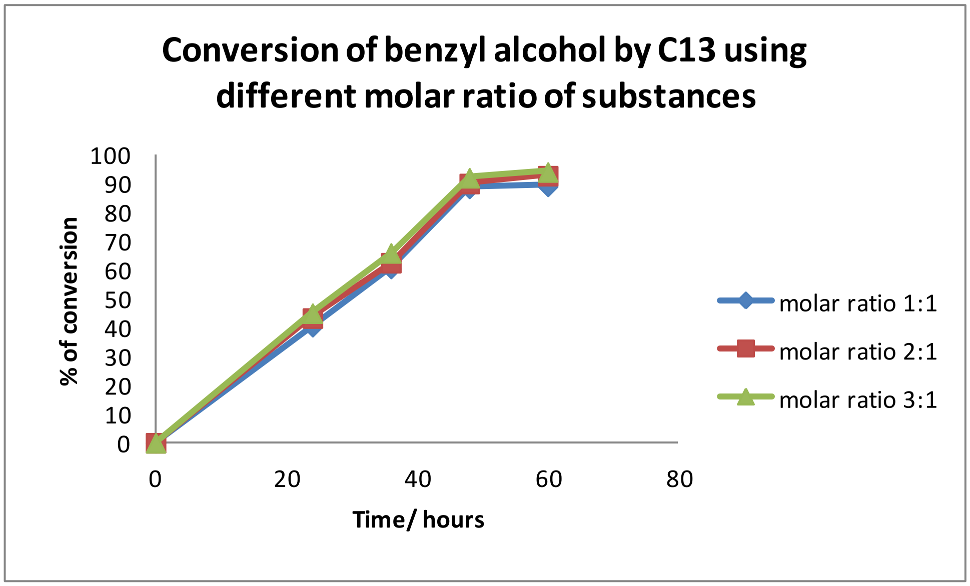

Figure 59: Conversion of benzyl alcohol by C13 using different molar ration of substance

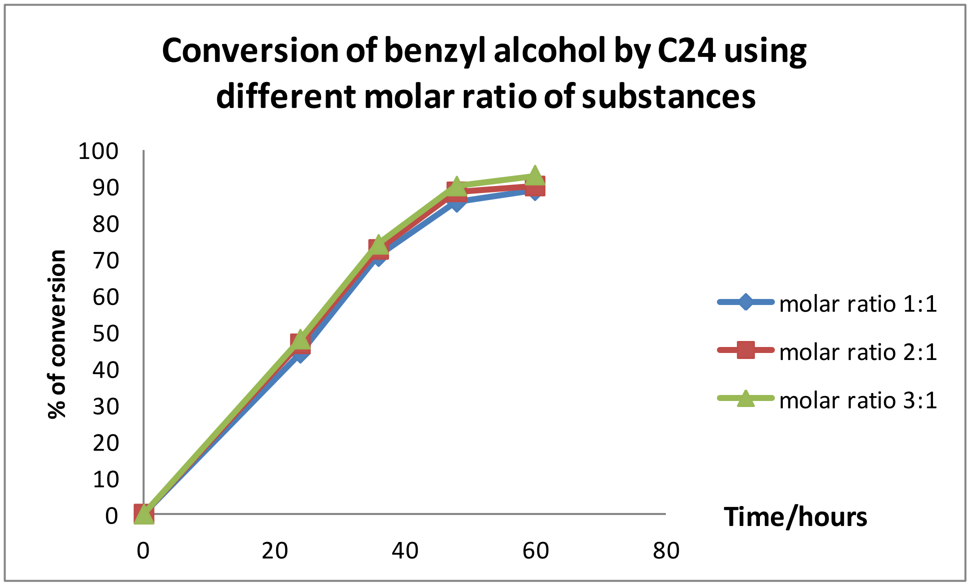

Figure 60: Conversion of benzyl alcohol by C24 using different molar ratio of substance

Description of the Influence of Concentration of Substrate on Catalytic Oxidation of Alcohol

The effect of molar ratio of benzyl alcohol/ H_2O_2 of 1:1, 2:1and 3:1 was studied using 2.0 mmol of catalysts at 90°C with vigorous stirring (table 44 % 45). Under the reaction condition mentioned, the molar ratio has no significant effect on the benzyl alcohol conversion. After 48 hours of reaction, the conversion of benzyl alcohol using molar ratio of 1:1 and 2:1 is 90%. With molar ratio 3:1, maximum conversion of benzyl alcohol to benzoic acid is achieved.

From the observation, the rate steadily increases when more substrate is added because more of the active sites of the enzyme are being used which results in more reactions so the required amount of oxygen is made more quickly. Once the amount of substrate molecules added exceeds the number of active sites available, then the rate of reaction will no longer improve. This is because active sites are not available when the reactions has exhausted.

3.8.5 Influence of Temperature

Table 46: Percentage of conversion of benzyl alcohol by **C13** at different temperatures

Temperature/°C	**Percentage of Conversion of Benzyl Alcohol by C13 at the First (Time/ hours)**					
	0	**24**	**36**	**48**	**60**	**72**
30	0	0	0	0	0	0
50	0	6.10	12.10	28.80	40.00	40.00
70	0	11.70	20.30	43.00	70.60	70.60
90	0	28.30	40.20	60.00	89.20	89.20
110	0	30.20	43.00	66.90	92.00	92.00
130	0	35.00	-	-	-	-

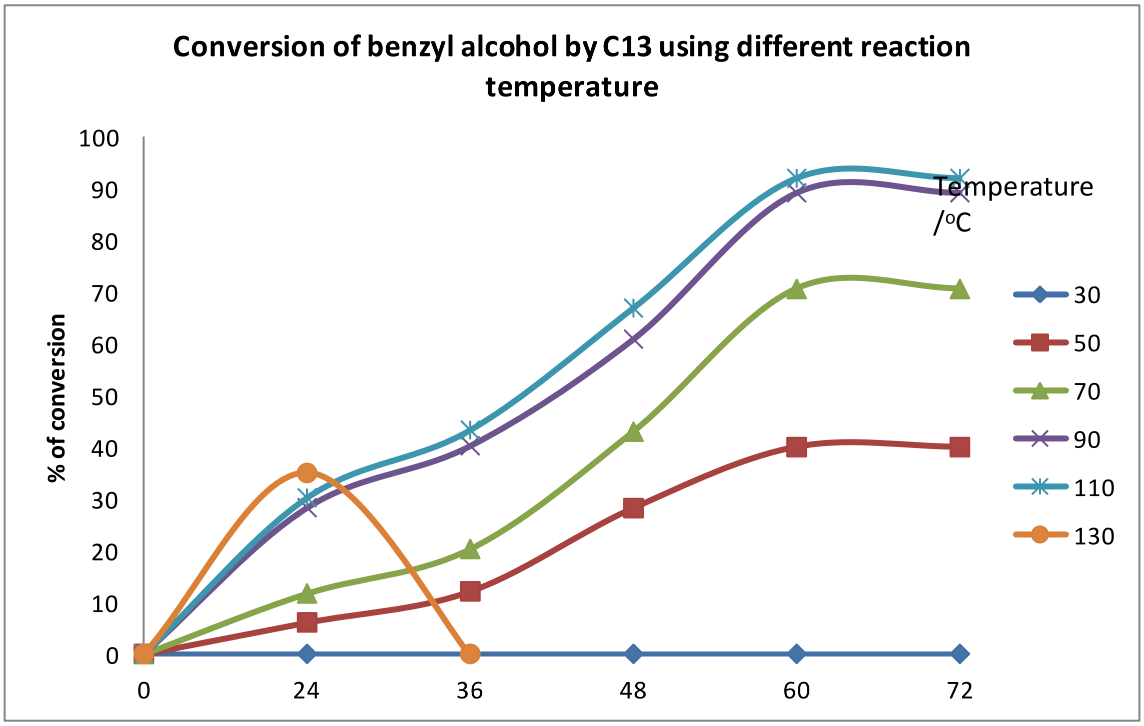

Figure 61: **Percentage of conversion of benzyl alcohol by C13 at different temperatures reaction Condition: Molar ratio of $C_6H_5CH_2OH/H_2O_2$ = 1:1; 0.001 mol of C13 at different reaction temperature up to 72 hours.**

Table 47: Percentage of conversion of benzyl alcohol by **C24** at different temperatures

Temperature/°C	**Percentage of Conversion of Benzyl Alcohol by C24 at the First (Time/ hours)**					
	0	**24**	**36**	**48**	**60**	**72**
30	0	0	0	0	0	0
50	0	15.30	33.10	45.00	62.20	62.20
70	0	32.60	48.90	57.10	72.30	72.30
90	0	40.20	60.90	79.90	87.90	87.90
110	0	43.30	66.80	82.00	90.00	90.00
130	0	45.00	68.30	84.20	90.20	90.20

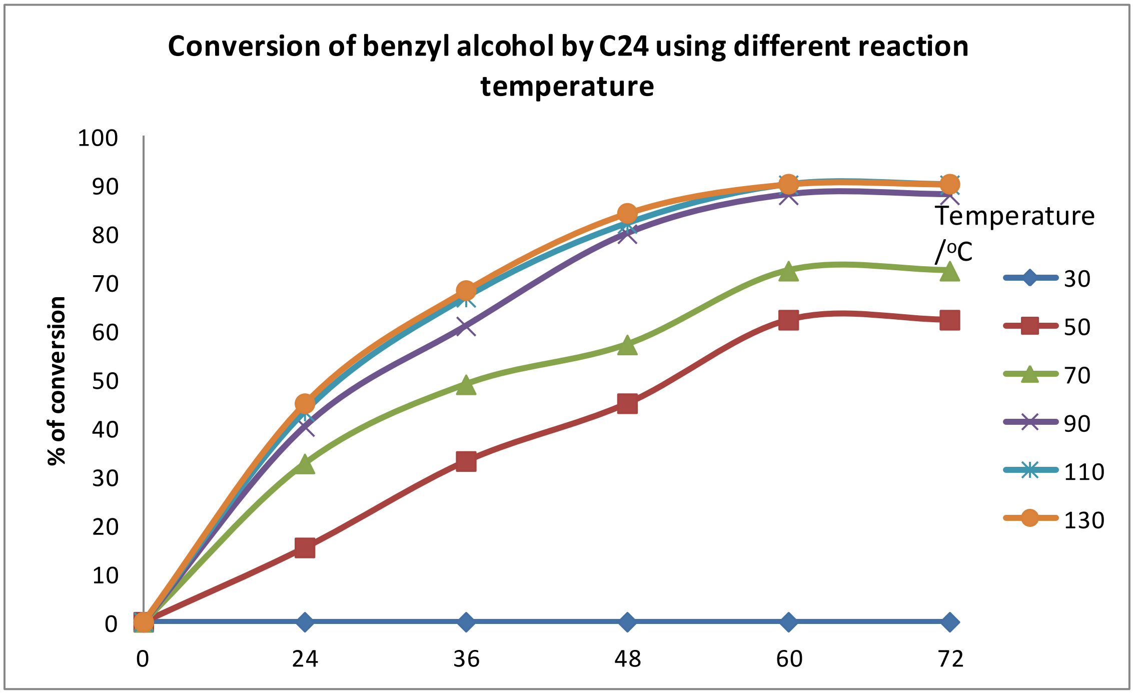

Figure 62: Percentage of conversion of benzyl alcohol by C13 at different temperatures. Reaction Condition: Molar ratio of $C_6H_5CH_2OH/H_2O_2$ = 1:1;0.001 mol of C24 at different reaction temperature up to hours.

Description of the Influence of Reaction Temperature

In catalytic oxidation, the effect of reaction temperature was significant. There was a great increment in the oxidation of benzyl alcohol when the reaction temperature is raised from 30 to 90°C by using **C13** and **C24** as the catalyst. A benzyl alcohol conversion of 90% was obtained at 90°C after 60 hours of reflux (table 46 & 47). There was not much effect when temperature was elevated from 90 to 110°C. For the reaction using **C13** and **C24** as catalysts, benzyl alcohol conversion of 89.20% and 87.90%, respectively, were obtained at 90°C after 60 hours of reflux. Thus, there was no need to raise the reaction temperature to 110°C as the total percentage of benzyl alcohol conversion differs only slightly. Furthermore, when the reaction temperature was brought to 130°C, **C13** undergoes decomposition after 36 hours of refluxing. This is corroborated by the thermal decomposition behaviour of **C13** from TGA analysis profiles that show **C13** started to dissociate at 130°C. Due to the different thermal stability of **C13** and **C24**, **C24** could be considered as an ideal catalyst in oxidation of alcohol as the catalyst can withstand a higher reaction temperature before it decomposes. It can be further concluded that the optimal temperature for catalytic oxidation using **C13** and **C24** is 90°C and 130°C respectively as a maximum amount of benzoic acid were obtained at these temperature.